

An enzyme-free amplification strategy based on two-photon fluorescent carbon dots for monitoring miR-9 in live neurons and brain tissues of Alzheimer's disease mice

Wenxiao Wu, Tingting Zheng* and Yang Tian*

Key Laboratory of Green Chemistry and Chemical Processes, Department of Chemistry, School of Chemistry and Molecular Engineering, East China Normal University Shanghai 200241 (P. R. China) E-mail: ttzheng@chem.ecnu.edu.cn; ytian@chem.ecnu.edu.cn.

Contents:

S1. Experimental Section

S2. Additional Figures

1. Sequence of DNA and miRNA (Table S1)
2. AFM image of CDs (Figure S1)
3. High resolution XPS characterization of CDs (Figure S2)
4. Detailed structure and characterization of DNA-Azo (Fig. S3)
5. The ratio of DNA-Azo to CDs in CDs-DNA-Azo (Fig. S4)
6. UV/Vis characterization (Figure S5)
7. Determination of percentage of azo groups that were transformed to the trans form (Fig. S6)
8. Morphology characterization of GO and M9 probe (Fig. S7)
9. Determination of The content ratio of CDs-DNA-Azo to GO in M9 probe (Fig. S8)
10. Investigation of TPE properties of M9 probe before and after addition of miR-9 (Fig. S9)
11. Response time experiment (Fig. S10)
12. Stability of the developed probe during detection of miR-9 (Fig. S11)
13. Competition and selectivity tests of the probe again other cellular compoments (Fig. S12)
14. Cytotoxicity and biocompatibility experiments of M9 probe in neurons (Figure S13)
15. RT-PCR experiments of miR-9 in neurons after incubation with various concentration of A β oligomer (Fig. S14)
16. Fluorescence imaging of hippocampus slices without M9 probe treatment (Fig. S15)

S1. Experimental section

Chemicals and materials. Thiourea, o-phenylenediamine and other reagents of certified analytical grade were obtained from Sigma-Aldrich (Shanghai, China). 3-(4, 5-dimethylthiazol-2-yl)-2, 5-diphenyltetrazolium bromide (MTT) was purchased from Beyotime Biotechnology (China). Annexin V-FITC apoptosis detection kit was obtained from Shanghai Sangon Biological Engineering Technology & Services Co. (Shanghai, China)., DNA, miRNAs and Beta-amyloid peptide (1–42) [A β (1–42)] were purchased from Sangon Biotech Co., Ltd (Shanghai, China). Lipofectamine-RNAiMAX transfection reagent, Opti-MEM, PureLink[®] RNA Mini Kit were obtained from ThermoFisher Scientific (MA, USA). Other solvents and reagents were used as received. All chemicals were of analytical grade and were used without further purification and modification. All samples were prepared by deionized water purified by Milli-Q. water purification system.

Apparatus and Instruments. Nuclear magnetic resonance (NMR) spectrum was recorded on a Bruker 500 MHz spectrometer (Bruker, Germany). The UV-Vis absorption spectrum and fluorescence spectrum were obtained with an UH5300 spectrophotometer (Hitachi, Japan) and F-4600 fluorescence spectrophotometer (Hitachi, Japan), respectively. High resolution transmission electron micrographs (HRTEM) images were taking using a JEM-2100 transmission electron microscope with an accelerating voltage of 200kV (JEOL, Japan). Atomic force microscope (AFM) image was recorded using the ScanAsyst mode with a Multimode Nanoscope IIIa atomic force microscope under ambient conditions (Bruker, Germany). AFM image was recorded with a Dimension Icon (Bruker, Germany). Fourier transform infrared spectroscopy (FT-IR) was obtained using a Thermo Scientific Fourier Transform Infrared spectrometer (Thermo Fisher scientific, USA). XPS data were performed on Thermo ESCALAB 250XI. The absorbance of cytotoxicity was recorded by a Varioskan LUX multimode microplate reader (Thermo Fisher scientific, USA). The apoptosis assay was conducted at a FACS Calibur flow cytometry (Becton, Dickinson and Company, USA). The fluorescence image and fluorescence lifetime imaging of cells were obtained from a Leica TCS SP8 confocal laser scanning microscope (Germany) equipped with two-photon laser (Chameleon Ultra II, Coherent).

Preparation and characterization of CDs. Thiourea and o-phenylenediamine were selected to facilitate the preparation of CDs. In brief, 200 mg Thiourea and 200 mg o-phenylenediamine were dispersed in 40 ml of deionized water under ultrasonication (500W, 40kHz). Subsequently, the mixture was transferred to a poly (tetrafluoroethylene) (Teflon)-lined autoclave (50 mL) and heated at 200 °C for 8 h. After cooled down to room temperature, the solution was filtered through a 0.22 µm microporous membrane and was further dialysed against deionized water for several times. Finally, CDs powder were obtained by the freeze-drying treatment for further use. Structures of CDs were characterized by High resolution transmission electron micrographs (HRTEM), Atomic force microscopy (AFM) and X-ray photoelectron spectroscopy (XPS).

Preparation and characterization of CDs-DNA-Azo and the probes for miR-9 (M9 probe, CDs-DNA-Azo@GO) The conjugation of DNA-Azo with CDs was carried out through chemical reaction between the aldehyde groups of CDs and the aldehyde groups of DNA-Azo. Briefly, CDs and DNA-Azo were mixed and stirred for 24 h at room temperature without light. After ultrafiltration (Millipore, 30 kDa, 6000 rpm, 10 min) three times to remove the unbound DNA, the CDs–DNA-Azo was collected, and diluted with 2.0 mL Tris buffer as a stock solution (5.0 mg mL⁻¹). As for M9 probe, the prepared CDs-DNA-Azo was further incubated with GO for another 2 h. Finally, washed with ultrapure water, the obtained probe was kept at 4 °C for the following fluorescence assays.

Detection of miR-9 in vitro. The M9 probe (50 µg/mL) was immersed in fresh cell lysis containing various concentrations of miR-9 from 4.0 fM~1.0 pM for further reacted 1 h at 37°C with water bath. After that, fluorescence signals of reacted solutions were excited at 960 nm two-photon wavelength and collected at 615 nm.

Preparation procedure of ROS. H₂O₂ was used as obtained. Hydroxyl radical (·OH) was generated by Fenton reaction (Fe²⁺/H₂O₂ =1:6). Peroxynitrite (ONOO⁻) was chemically produced by H₂O₂ and NaNO₂. Superoxide anion O₂^{·-} was generated by dissolving KO₂ in the DMSO solution. The concentration of O₂^{·-} was determined by measuring the reduction of ferricytochrome c spectrophotometrically using an

UV-vis spectrophotometer and the extinction coefficient of ferrocytochrome c at 550 nm ($21.1 \text{ mM}^{-1} \text{ cm}^{-1}$).

Cytotoxicity and biocompatibility of the nanosensor. Neurons were seeded in a 96-well cell culture plate 24 h prior to material treatments at a density of 1×10^4 cells/well. After the incubation of 24 h, neurons were treated with the prepared probe of specific concentrations at 37°C , 5% CO_2 for 6 h, respectively. Cytotoxicity was determined by performing the MTT assay. Briefly, $10 \mu\text{L}$ of MTT solution (10 mg/mL) was added into each well, and incubating for another 4 h, after washed with PBS, $80 \mu\text{L}$ of DMSO was added to terminate the reaction. Absorbance at 490 nm was measured through a Varioskan LUX-multimode microplate reader (Thermo Fisher Scientific, USA). Cell viability was determined by calculating the absorbance result. Cell viability (%) = the absorbance of experimental group/the absorbance of blank control group $\times 100\%$. For biocompatibility test, after incubation with the prepared probe, neurons were stained with Annexin V-FITC/PI, rinsed with PBS and resuspended in sequence according to the manufacturer's instruction. Finally, the collected solution was performed with flow cytometric assay using Cytomics FC500 Flow Cytometry (Beckman Coulter Ltd.). All experiments detected at least 8000 cells, and the data were analyzed using FCS Express V3.

Co-localization experiment of M9 probe in neurons. Neurons were placed onto 35 mm plastic Petri dishes with 20 mm bottom well and cultivated for 20 h. After removing the cultured solution, neurons were washed three times with PBS buffer, fresh cell medium containing the probe at the concentration of $50 \mu\text{g/mL}$ was added into the well and further incubated for 3 h. After that, M9 probe-labeled neurons were further stained with 100 nM cell tracker for 20 min. Following by that, neurons were washed thrice with PBS buffer to imaging. Fluorescence imaging of cell Tracker blue were acquired with a 405 nm excitation laser, while for the prepared probes, it was excited at two photon 960 nm.

Preparation of A β oligomer. A β_{1-42} was dissolved in 1, 1, 1, 3, 3, 3-hexafluoro-2-propanol (HFIP) to a concentration of 1 mg/mL . Then, the solution was shaking at 4°C for 2 h at room temperature. The obtained sample was stored at -20°C as stocked solution. Immediately prior to use, the HFIP was removed

by evaporation under a gentle stream of nitrogen and the peptides were dissolved in distilled, deionized water. By mixing an aliquot of the peptides and CuCl₂ at a molar ratio of 1:1 into 10 mM HEPES (150 mM NaCl, pH 6.6) at 37°C for 32 h, Cu²⁺ induced aggregation of Aβ₁₋₄₂ was accomplished.

Flow cytometric assay. Neurons were seeded in a 6-well plate and incubated in complete medium for 24 h at 37°C, 5% CO₂. After washed three times with PBS buffer, neurons were treated with 0, 10, 20, 50 μM Aβ oligomer for 20 h. Followed by rinsed, neurons were harvested, stained with Annexin V-FITC/PI according to the manufacturer's instruction, rinsed with PBS, resuspended, and subjected to perform flow cytometric assay using Cytomics FC500 Flow Cytometry (Beckman Coulter Ltd.). All experiments detected at least 8000 cells, and the data were analyzed using FCS Express V3.

RT-PCR analysis of miR-9 in neurons. Neurons were seeded in a 6-well plate and incubated in complete medium for 24 h at 37°C, 5% CO₂. After washed three times with PBS buffer, neurons were treated with 0, 10, 20, 50 μM Aβ oligomer for 20 h. The levels of miR-9 in total RNA extracted from neurons were determined using a miRNA specific qRT-PCR kit. The PureLink[®]RNA Mini Kit was used for isolating total RNA. The TaqMan MicroRNA Reverse Transcription Kit was used for performing reverse transcription reaction. The 15 μL RT reaction mixture was consisted of 7 μL, RT master mix, 5 μL, total RNA sample (10 ng), or the desired amount of synthetic miR-9 for the standards, and 3 μL of 5×RT primer solution. For the reverse transcription reaction, each sample and the blank were performed in triplicate. The RT reaction program was: 16°C, 30 min, 42°C, 30 min, 85°C, 5 min, and then held at 0 °C. cDNA was amplified by PCR using the miR-9 specific TaqMan MicroRNA Assay.

Two-photon fluorescence imaging of miR-9 in Aβ-treated neurons using the developed M9 probe.

Neurons were incubated with as-prepared Aβ oligomer for 20 h, and then incubated with the prepared probe (50 μg/mL) for 3 h under 5% CO₂ atmosphere at 37 °C. Then the solution was removed and the cells were washed with phosphate-buffered saline (PBS) for three times. The average fluorescence intensity was obtained neuron by neuron, where 10 neurons in each condition were evaluated after stimulated by various Aβ oligomer. Fluorescence images was performed on a TCS-SP8 confocal laser-scanning

microscope (Leica) equipped with two-photon laser (Chameleon Ultra II, Coherent) using a 63× glycerol immersion objective (NA 1.4) (ex = 960 nm).

Preparation, staining of fresh mouse hippocampal slices and two-photon fluorescence imaging of miR-

9 in hippocampal tissues. Wide type, 6, and 15 months-old mice (APP.PS1) with AD were purchased from the Laboratory Animal Center of the Chinese Academy of Science. Mice hippocampal slices were obtained with the thickness of 450 μm using a vibrating-blade microtome (Leica VT3000). Then, the slices were immersed in ice artificial cerebrospinal fluid (ACSF) (124 mM NaCl, 3 mM KCl, 26 mM NaHCO₃, 1.25 mM NaH₂PO₄, 10 mM D-glucose, 2.4 mM CaCl₂, and 1.3 mM MgSO₄) to control excessive neuronal excitation, and then transferred to an incubation chamber filled with aCSF containing 50 μg/mL M9 probe, 95% O₂ and 5% CO₂ for 4 h at 37 °C. Finally, all slices were washed three times with ACSF and put into a new chamber for fluorescence imaging with ×10 dry, ×63 oil objectives under the excitation of 960 nm. Fluorescence intensity was collected at each region of interest (ROI), where 10 ROIs in 10 brain tissues from each normal or AD mice were measured. After that, average fluorescence intensity of the images was obtained.

S2. Additional Figures.

1. Sequences of DNA and miRNA (Table S1)

Table S1. Sequences of DNA and miRNA

name	Sequences(5'-3')
DNA-Azo	CHO-(CH ₂) ₆ CCTAGCTCATACAGCTAGATAACCAAAGA(Azo)GC(Azo)TA(Azo)GG
MiRNA-9	UCUUUGGUUAUCUAGCUGUAUGA

2. AFM image of CDs (Figure S1)

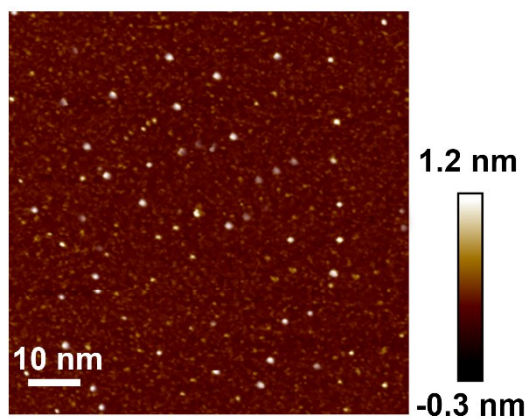


Fig. S1 AFM image of the prepared CDs.

3. High resolution XPS characterization of CDs (Figure S2)

Three typical peaks: C 1s (285 eV), N 1s (400 eV), and O 1s (531 eV) were observed from XPS experiments (Fig. S2). In high-resolution XPS N 1s, fitting peaks at 399.85 and 400.8 eV are corresponding to the pyrrolic-like N and graphitic-like/amino N, respectively.

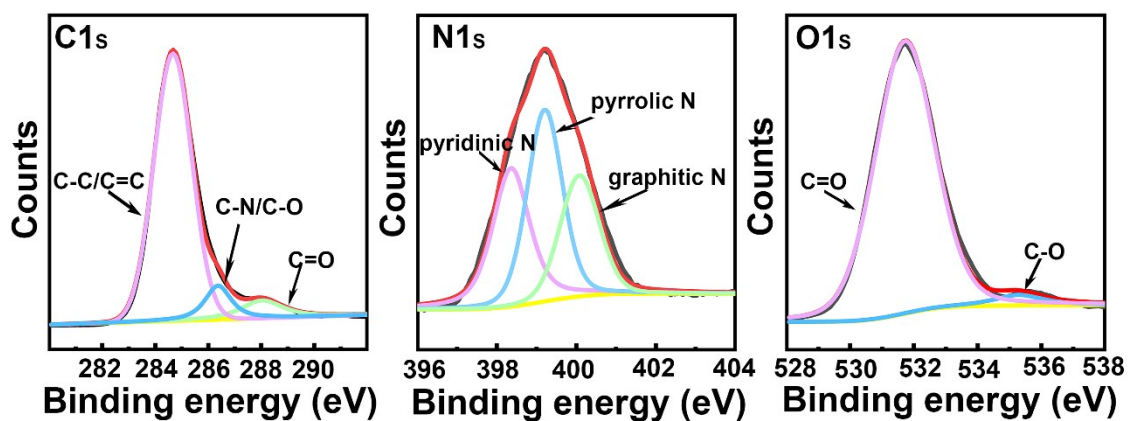


Fig. S2 High resolution XPS characterization of CDs.

4. Detailed structure and characterization of DNA-Azo (Fig. S3)

DNA-Azo were provided by Sangon Biotech Co., Ltd (Shanghai, China). The structure of aldehyde groups modification (CHO) on the 5' of DNA and the embedded Azo unit were depicted in Fig. S3a and S3b, respectively. The molecular weight (MW) of the DNA embedded with Azo was calculated to be 11867.97. After modified with CHO (MW: 228.10), the final MW of DNA-Azo was calculated to be 12096.07, which was confirmed by the mass spectrum result (MW: 12097.6, Fig. S3c), suggesting the successful preparation of DNA-Azo in this work.

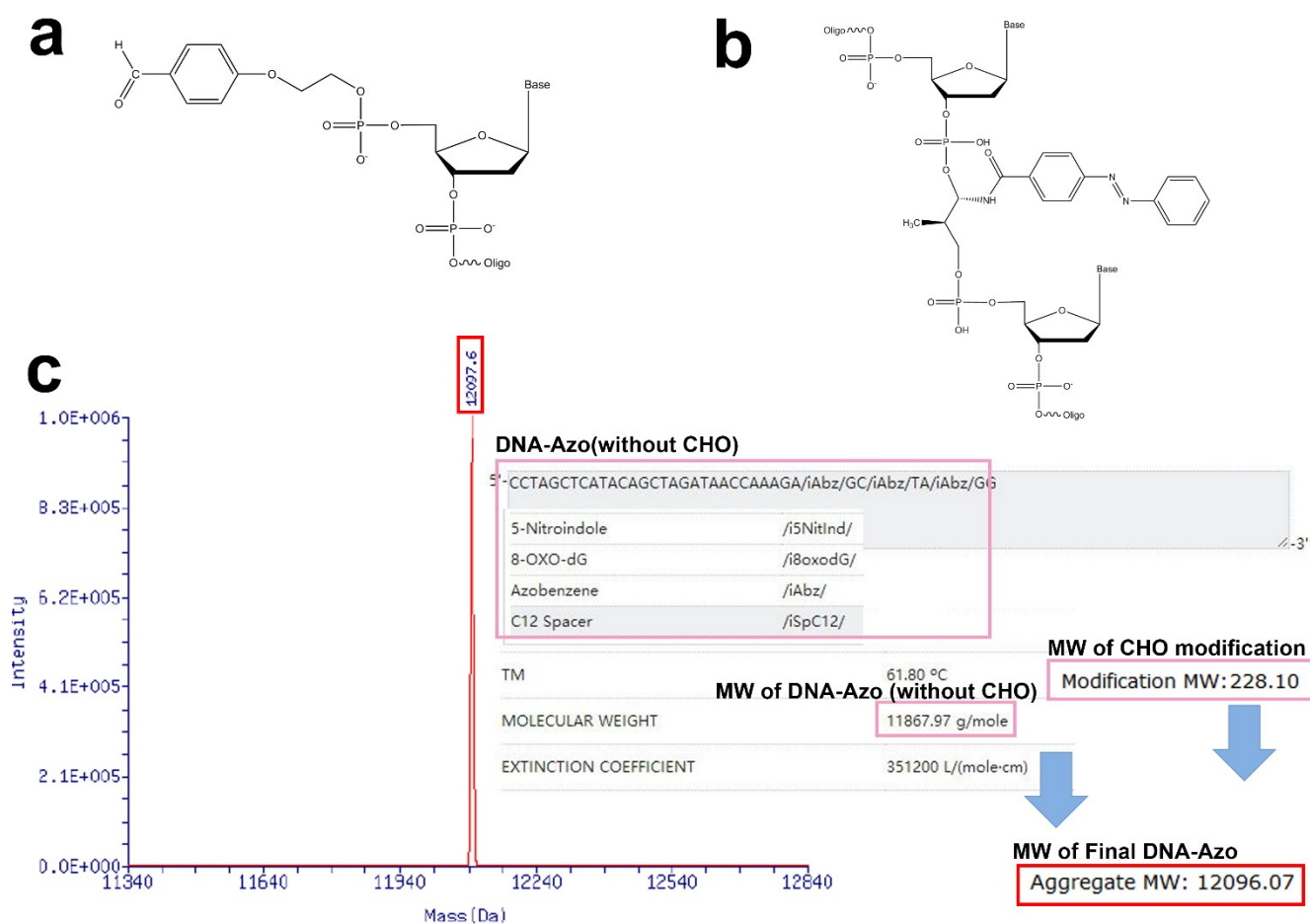


Fig. S3 a) The structure of -CHO modification on the 5' of DNA. b) The structure of the embedded Azo unit in this DNA sequence. c) Mass characterization and theoretically calculated data of the DNA sequence in this work.

5. The ratio of DNA-Azo to CDs in CDs-DNA-Azo (Fig. S4)

Firstly, since DNA-Azo was chemically modified onto CDs as CDs-DNA-Azo, the DNA-Azo in CDs-DNA-Azo was estimated by subtracting the amount of DNA-Azo in the supernatant from the total amount of DNA-Azo (200 μM , 112 μL , 272 μg) added into the CDs solution (0.1 mg/mL, 10 mL, 1 mg). To determine the amount of DNA-Azo in the supernatant, absorbance (A) - concentration (c) standard curves were investigated by recording the absorbance of various concentrations of DNA-Azo (1, 3, 5, 7, 9 and 11 μM). As shown in Fig. S4a, characteristic absorption of DNA and Azo appeared at 260 and 340 nm, respectively (Anal. Chem. 2017, 89, 1704–1709; J. Am. Chem. Soc. 2019, 141, 8239–8243), and the absorbances at each peak were increased with the increasing concentration of DNA-Azo. Therefore, the relationship between A ($\lambda_{260\text{ nm}}$) and c of DNA-Azo was obtained as the equation of $A=0.01c+0.03$ (Fig. S4b). Since the A ($\lambda_{260\text{ nm}}$) of DNA-Azo in the supernatant was measured to be 0.041, the amount of DNA-Azo in the supernatant was calculated to be 1.1 μM (1mL, 13.4 μg) according to the equation. And the DNA-Azo in CDs-DNA-Azo was calculated to be 258.6 μg , so the ratio of DNA-Azo to CDs was calculated to be 0.26:1 (mass concentration ratio).

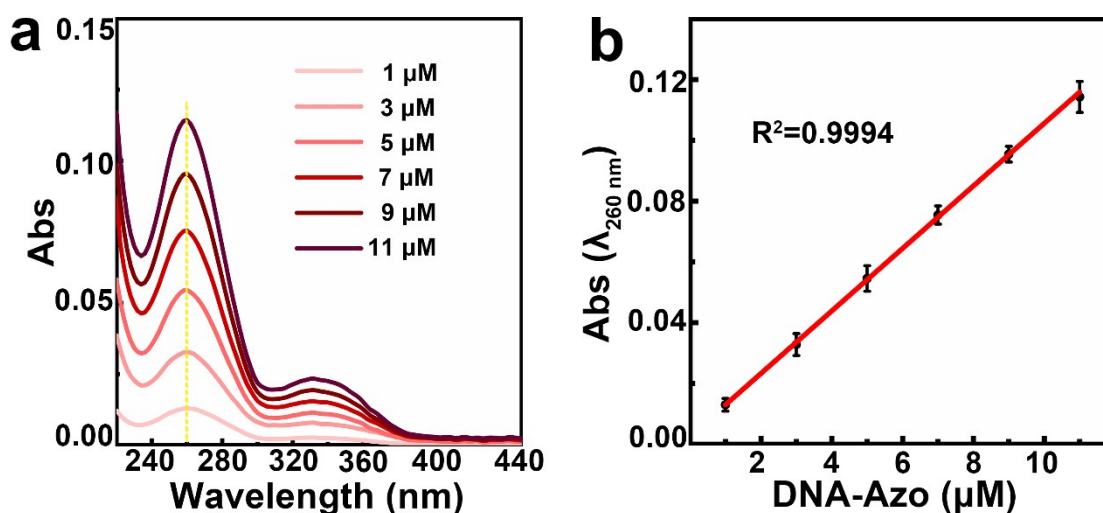


Fig. S4 a) UV-vis spectra of DNA-Azo at various concentration from 1 to 11 μM , b) Liner relation between absorbance at 260 nm (A) and the concentration of DNA-Azo (c), $A=0.01c+0.03$ ($R^2=0.9994$), (Error bars: S. D., $n = 6$).

6. UV/Vis characterization of CDs-DNA-Azo (Fig. S5)

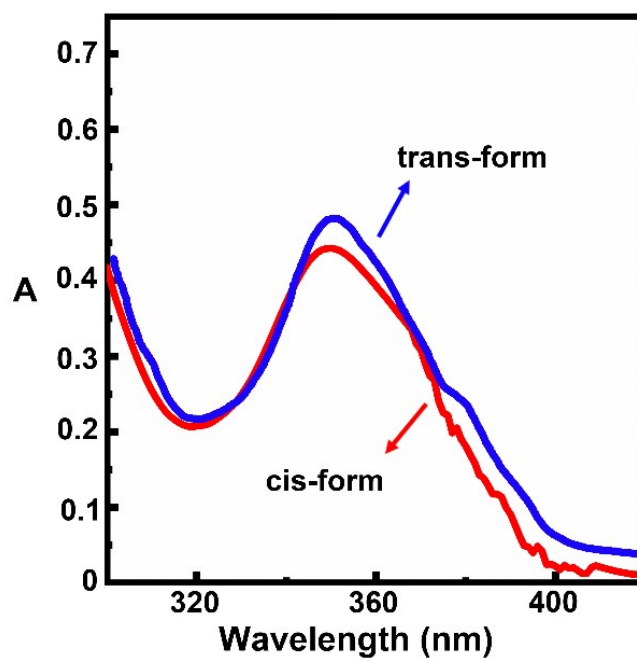


Fig. S5. Absorption spectra change of CDs-DNA-Azo between from cis- to trans-, induced by the emission of CDs.

7. Determination of percentage of azo groups that were transformed to the trans form (Fig. S6)

Since no obvious peak of cis form DNA-Azo groups (under UV light) was observed in circular dichroism spectrum (Fig. 1d), the percentage of azo groups that were transformed to the trans form was estimated through transformed of DNA-Azo divided by the totally complete trans form of DNA-Azo.

As previously reported, there are featured absorption peaks of Azo at 340 nm (UV, cis form) and 450 nm (Vis, trans form) (Adv. Mater. 2018, 1804982), thus the complete trans-form DNA-Azo was obtained at first through irradiating at 450 nm for 5 min. As shown in Fig. S6, the circular dichroism spectrum showed that the complete trans form DNA-Azo (purple line) exhibited negative and positive bands at 248 nm and 277 nm, respectively.

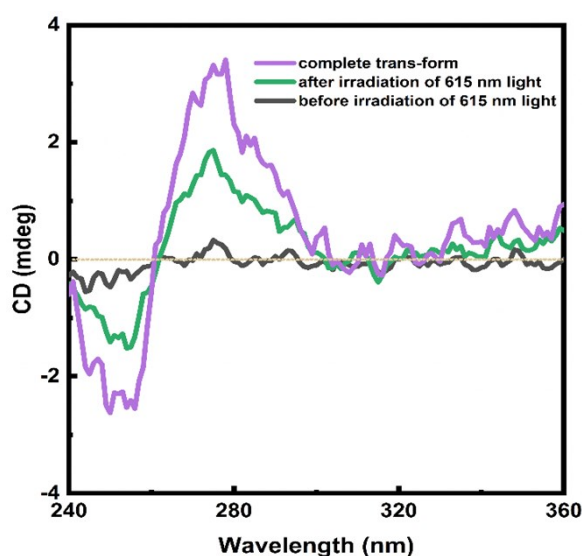


Fig. S6 Circular dichroism spectra of the complete trans-form DNA-Azo (purple line) and DNA-Azo before (gray line) and after irradiation of 615 nm light.

When exposed to 615 nm light for 5 min (green line), the DNA-Azo was partially transformed to trans form, and also showed the same negative and positive bands in circular dichroism spectrum. In this case, the transformed percentage was obtained by the peak value ratio of transformed trans form to complete trans form at 277 nm (or 248 nm). The peak value at 277 nm of transformed trans form were 1.89, and complete trans form was 3.56, so percentage of Azo groups that were transformed to the trans form was calculated to 0.52 (1.89/3.56).

8. Morphology characterization of GO and M9 probe (Fig. S7)

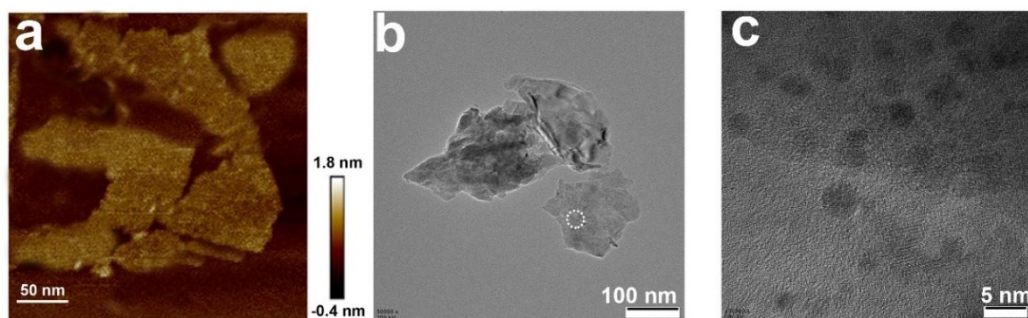


Fig. S7 a) AFM characterization of GO. TEM characterization of the b) prepared probe and c) partial enlargement images, which indicated the CDs on the surface of GO.

9. Determination of The content ratio of CDs-DNA-Azo to GO in M9 probe (Fig. S8)

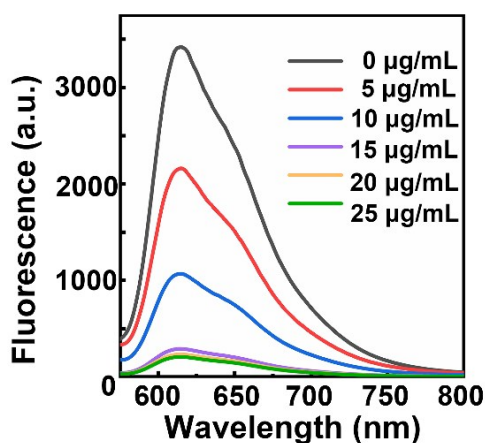


Fig. S8 Fluorescence spectra of CDs-DNA-Azo after incubated with various concentration of GO (0, 5, 10, 15, 20, and 25 $\mu\text{g/mL}$).

CDs-DNA-Azo and GO were employed to establish M9 probe by π - π stacking. For optimizing the concentration of GO, CDs-DNA-Azo (0.1 mg/mL, 10 mL) was mixed with various concentrations of GO (0, 5, 10, 15, 20 and 25 $\mu\text{g/mL}$) in Tris-HCl buffer solution (20 mM Tris, 100 mM NaCl, 5 mM KCl, and 1 mM MgCl_2). The above solutions were allowed to incubate for 10 min, and then the fluorescence intensities were recorded at 615 nm. Due to the quenching effect of GO, the fluorescence of CDs-DNA-Azo was gradually decreased as the concentration of GO increased, and the concentration of GO was optimized to 15 $\mu\text{g/mL}$ (Fig. S8). Therefore, the content ratio of GO to CDs-DNA-Azo in M9 probe was calculated to 0.15:1 (mass concentration ratio).

10. Investigation of TPE properties of M9 probe before and after addition of miR-9 (Fig. S9)

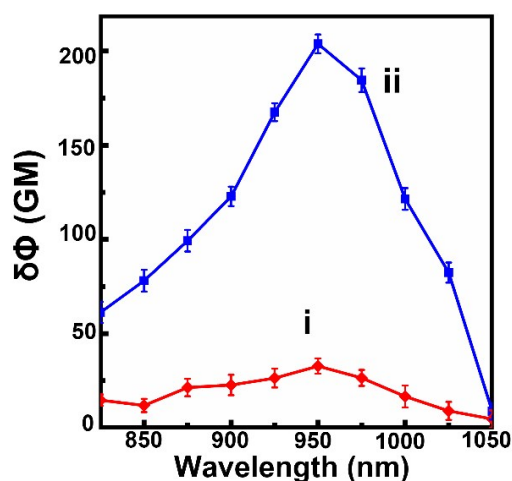


Fig. S9 Two-photon action spectra of M9 probe (50 $\mu\text{g}/\text{mL}$) (i) before (red line) and after the addition of (ii) miR-9 (100 fM, blue line) (Error bars: S. D., $n = 6$).

11. Response time experiment (Fig. S10)

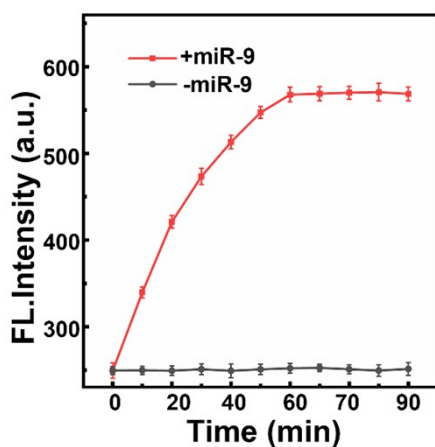


Fig. S10 Response time experiment, fluorescence intensity changes of M9 probe before and after reacting with 8.0 fM miR-9 from 0 to 90 min in cell lysis, (Error bars: S. D., $n = 6$).

After the addition of miR-9 (8.0 fM), fluorescence of the probe gradually increased and finally reached to a plateau, and the responsive time was optimized to 1 h. In comparison, the blank sample (missing the miR-9) showed only a very marginal increase in fluorescence signal which confirmed the proposed detection strategy.

12. Stability of the developed probe during detection of miR-9 (Fig. S11)

Fluorescence changes of the developed probe against various pH (4.0, 5.0, 6.0, 7.0, 8.0, and 9.0) for 70 min were investigated. In the absence of miR-9 (Fig. S11a), the M9 probe appeared fluorescence signal recovery in strong acid (pH<6) or alkaline environment (pH>8). It was attributed to the hydrolyzed and denaturation of DNA causing the lessened conjugation of CDs-DNA-Azo and GO (Biopolymers 1969, 8, 559-571). After reacting with miR-9 (0.1 pM) for 1 h (Fig. S11b), it was observed that the fluorescence intensity of M9 probe still continuously increased at pH 4.0, 5.0 and 9.0, indicating the denaturation of DNA as well as disturbed base pairing (Biopolymers 1969, 8, 559-571). But overall, at pH 6-8, which was close to the physiological environment, the probe was stable to detect miR-9 within the signal response time (60 min).

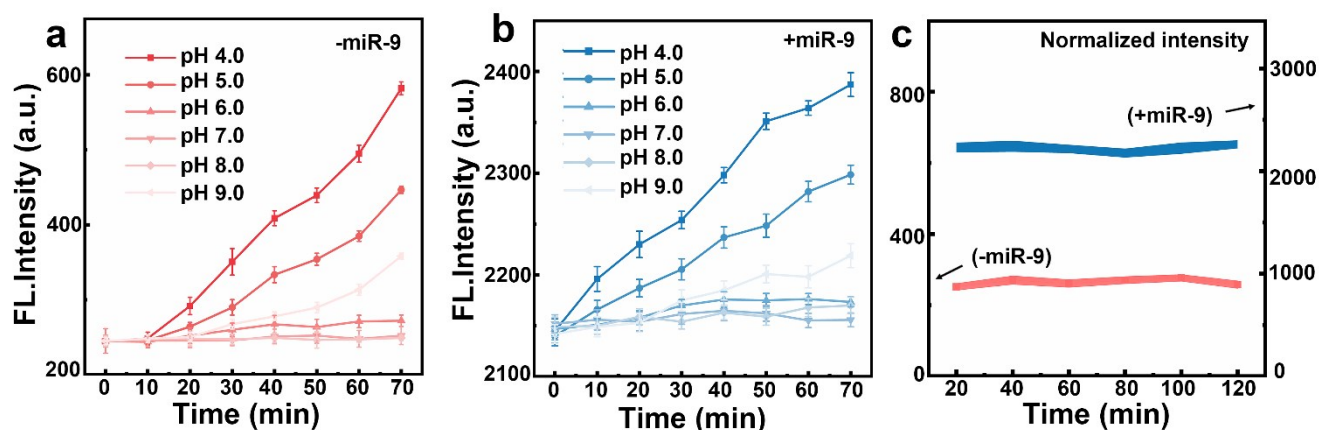


Fig. S11 pH stability tests (4.0-9.0) of the developed M9 probe before a) and after b) reacting with 100 fM miR-9. c) photostability test of the prepared M9 probe (50 $\mu\text{g}/\text{mL}$) in response to 100 fM miR-9 in cell lysis under 90 W xenon lamp to about 2 h (Error bars: S. D., $n = 6$).

13. Competition and selectivity tests of the probe again other cellular components (Fig. S12)

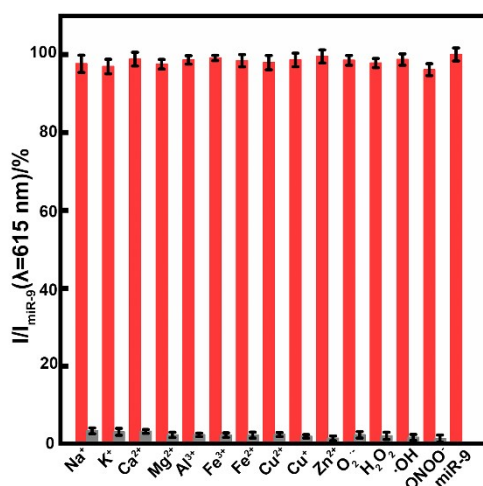


Fig. S12 Selectivity and competition tests of the M9 probe toward various (a, b) metal ions (1.0 mM for Na^+ , K^+ , Ca^{2+} , and Mg^{2+} ; 100 μM for Fe^{3+} , Fe^{2+} , Cu^{2+} , Cu^+ and Zn^{2+}), ROS (100 μM for $\text{O}_2^{\bullet-}$, H_2O_2 , $\bullet\text{OH}$, ONOO^-); Gray bars represent one of these interferents was added to the M9 probe solution (50 $\mu\text{g}/\text{mL}$). The red bars show both miR-9 (40 fM) and one of the competing species were added into the probe solution. Measurement conditions: $\lambda_{\text{ex}} = 960 \text{ nm}$, $\text{pH} = 7.4$, fresh cell lysis, (Error bars: S. D., $n = 6$).

14. Cytotoxicity and biocompatibility experiments of M9 probe in neurons (Figure S13)

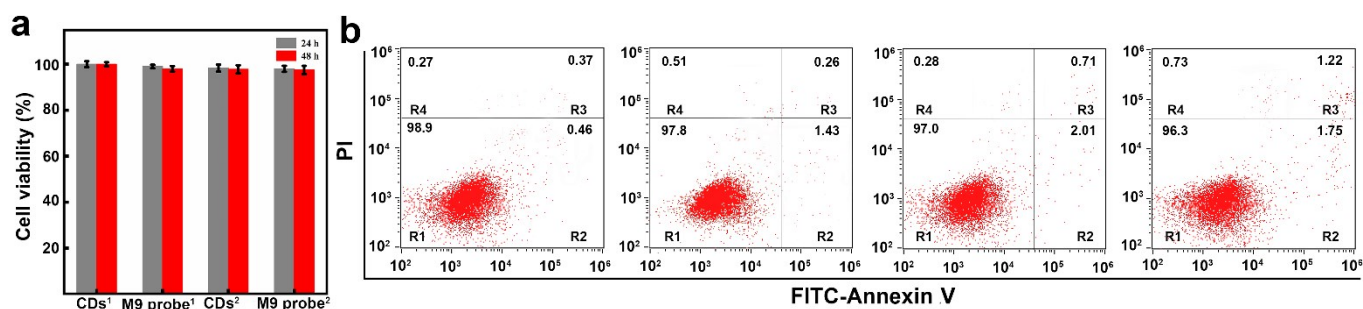


Fig. S13 a) MTT experiments and b) flow cytometry apoptosis assay. R1, R2, R3, and R4 represents the region of normal cells, early apoptotic cells, late apoptotic cells, and dead cells, respectively. From left to right: neurons were incubated with the CDs, M9 probe at the concentrations of 50, 50, 100 and 100 $\mu\text{g}/\text{mL}$, respectively.

15. RT-PCR experiments of miR-9 in neurons after incubation with various concentration of $\text{A}\beta$ oligomer (Fig. S14)

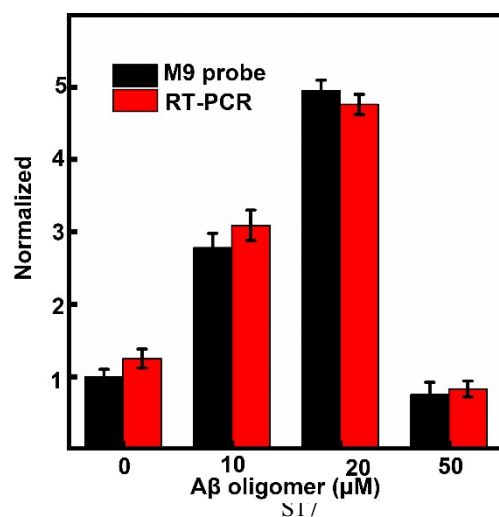


Fig. S14 The results comparison of miR-9 in neurons treated with A β oligomer using M9 probe fluorescence assay (black) and RT-PCR (red), (Error bars: S. D., n = 6).

16. Fluorescence imaging of hippocampus slices without M9 probe treatment (Fig. S15)

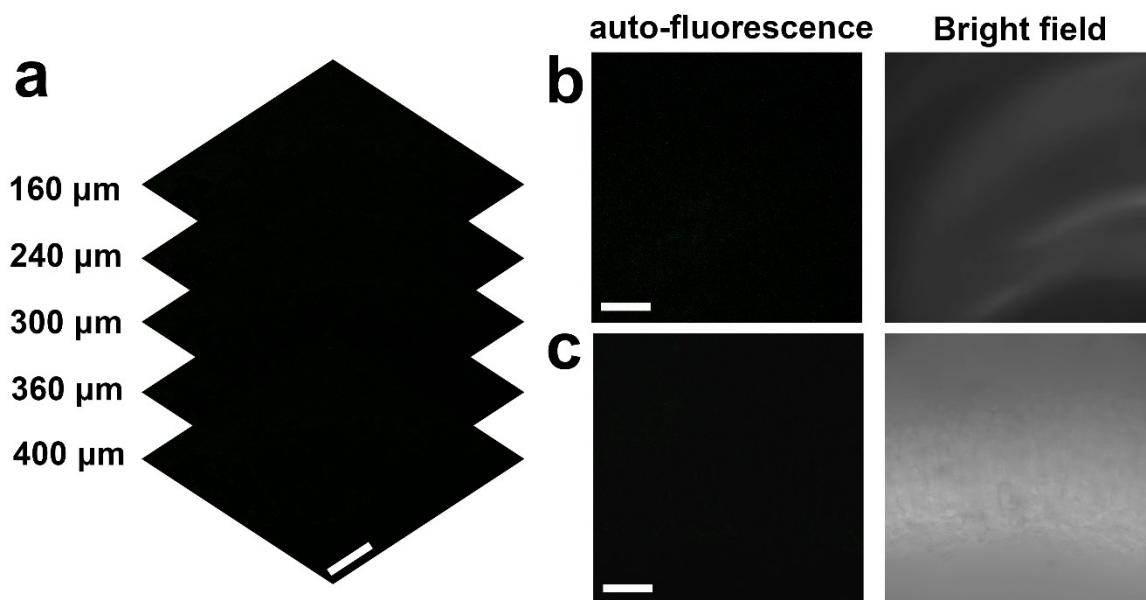


Fig. S15 a) Two-photon fluorescence imaging of hippocampus slices with z-stacking scanning without M9 probe treatment. Scale bar: 100 μm . b) and c) Two-photon fluorescence images of hippocampus slices images without M9 probe treatment, scale bar: 500 and 25 μm , respectively. Excitation wavelength: 960 nm.